Supporting Information

Constructing built-in electric field in 2D/2D Schottky heterojunction for efficient alkaline seawater electrolysis

Hongjun Chen,[a] Liming Deng,[a] Sheng Zhao,[a] Shuyi Liu,[a] Feng Hu,*[a] Linlin Li,*[a] Jianwei Ren[b] and Shengjie Peng*[ac]

[a] College of Materials Science and Technology, Nanjing University of Aeronautics and Astronautics, Nanjing 210016, China

E-mail: fenghu@nuaa.edu.cn (Feng Hu), lilinlin@nuaa.edu.cn (Linlin Li), pengshengjie@nuaa.edu.cn (Shengjie Peng)

[b] Department of Mechanical Engineering Science, University of Johannesburg, 2092 Johannesburg, South Africa

[c] State Key Laboratory of High Performance Ceramics and Superfine Microstructure

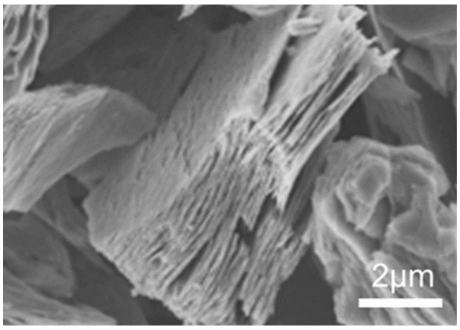

Fig. S1. SEM image of multilayer MXene.

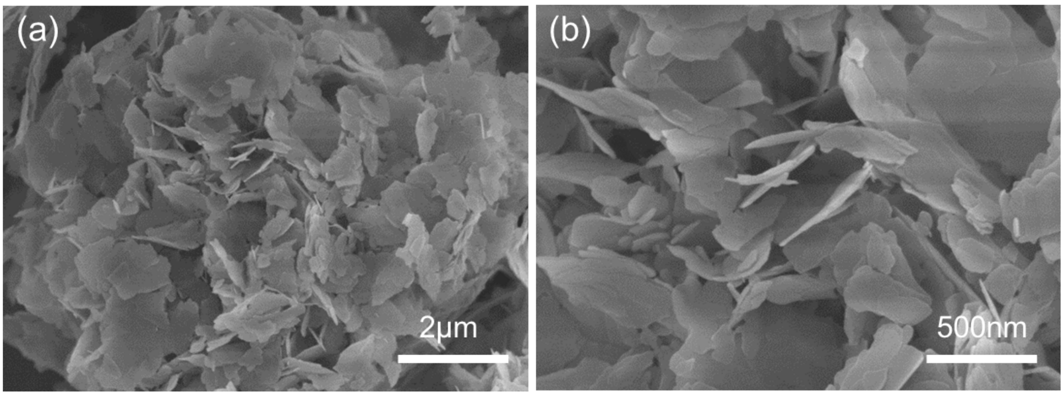

Fig. S2. (a) High-power; (b) low-power SEM images of $Co_3(PO_4)_2$.

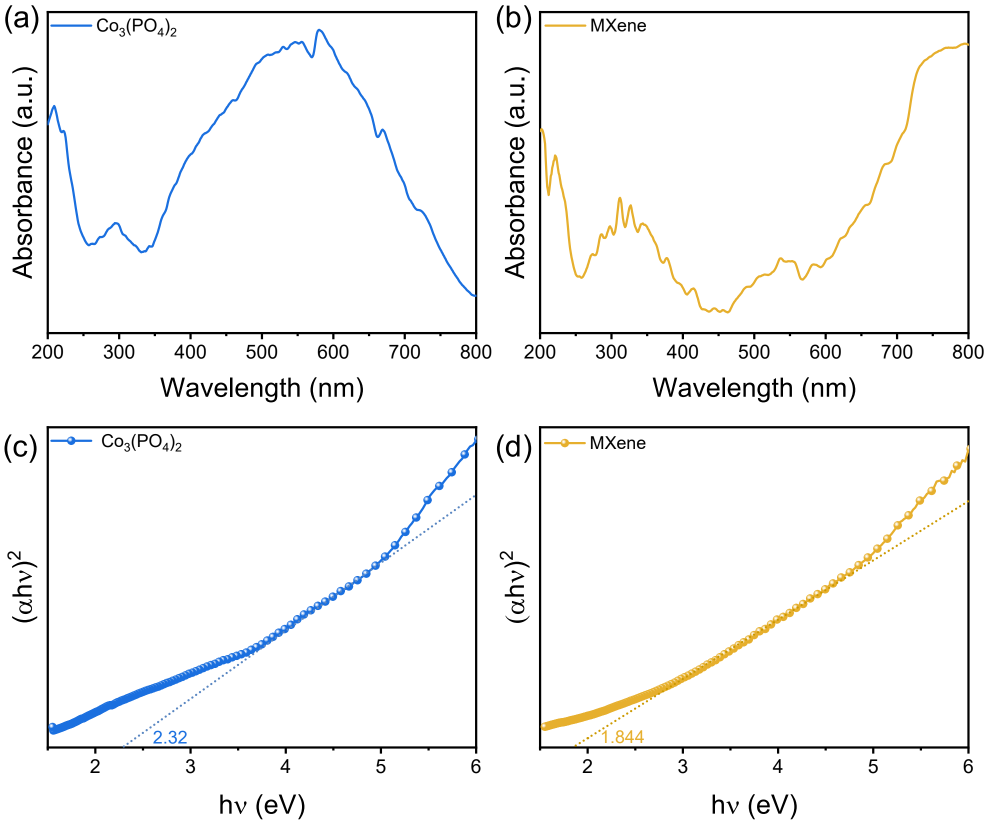

Fig. S3. Tauc plots converted from UV–vis diffuse reflection spectra of $Co_3(PO_4)_2$ and MXene.

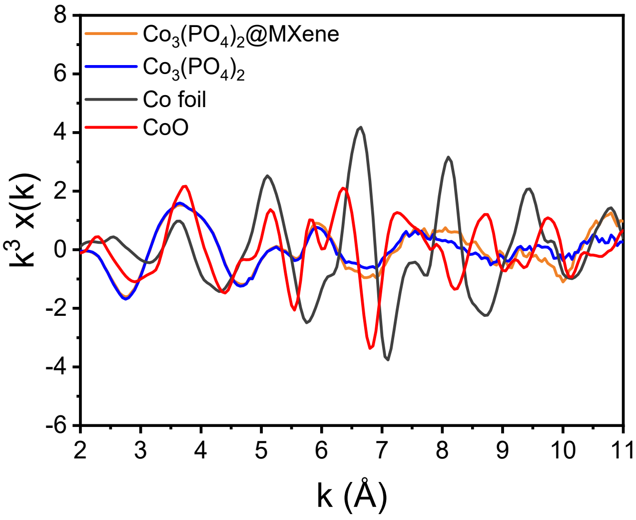

Fig. S4. Co K-edge EXAFS oscillation function of Co foil, CoO, $Co_3(PO_4)_2$ and $Co_3(PO_4)_2$@MXene.

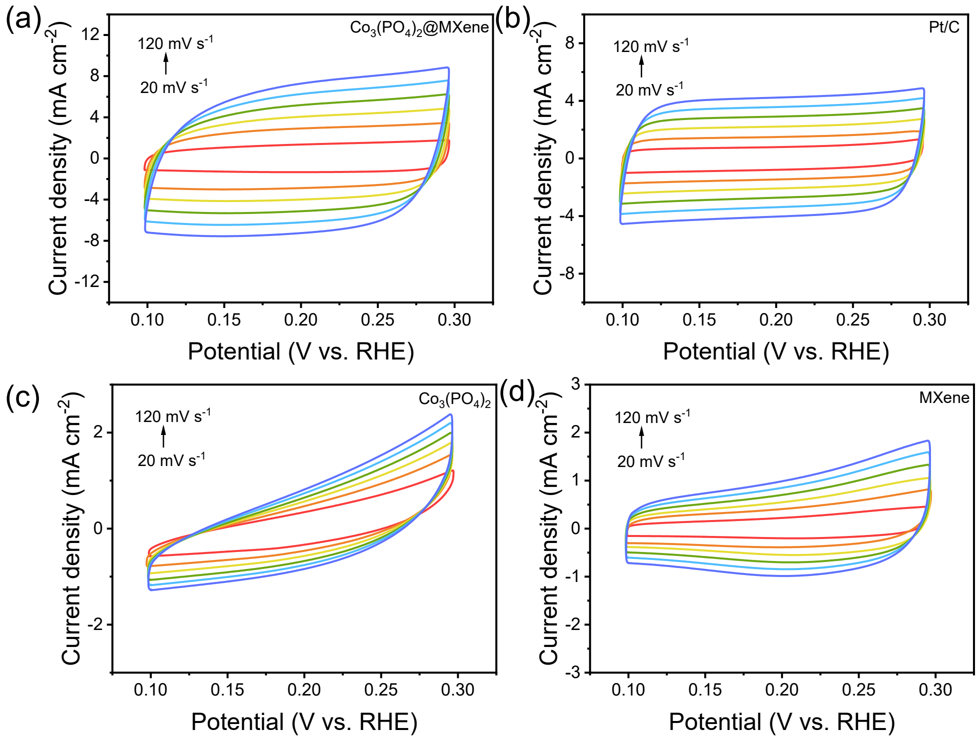

Fig. S5. Cyclic voltammetry of (a) $Co_3(PO_4)_2$@MXene, (b) Pt/C, (c) $Co_3(PO_4)_2$, and (d) MXene at different scanning rates (20, 40, 60, 80, 100, and 120 mV s^{-1}) in the range of 0.1~ 0.3 V vs. RHE potentials, used to estimate double layer capacitance (C_{dl}).

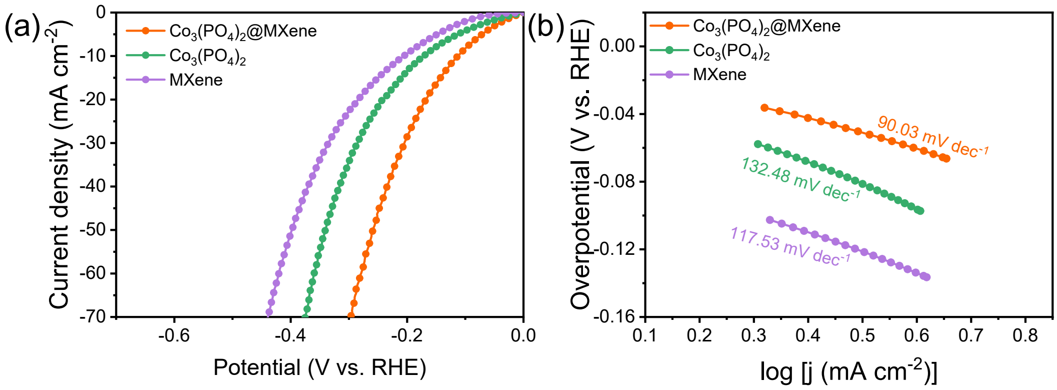

Fig. S6. (a) LSV polarization diagram, (b) Tafel slope diagram of $Co_3(PO_4)_2$, MXene and $Co_3(PO_4)_2$@MXene in seawater electrolyte.

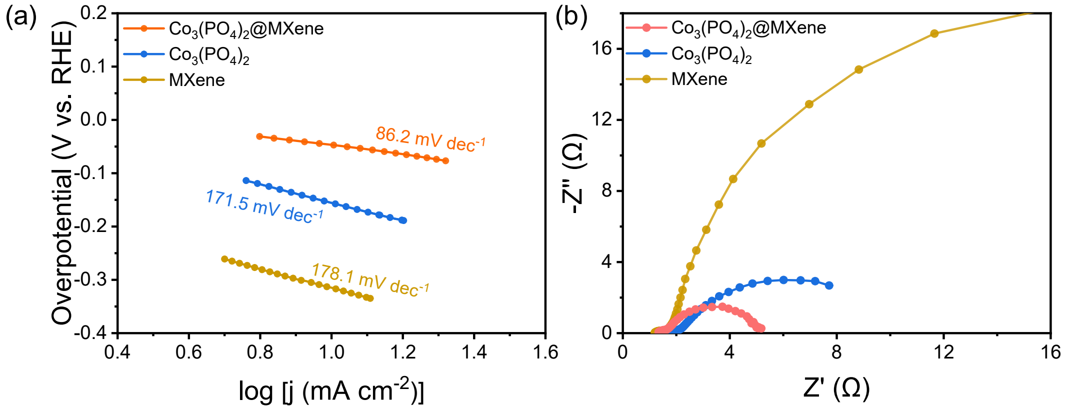

Fig. S7. (a) Tafel slope diagram, (b) EIS curves of $Co_3(PO_4)_2$, MXene and $Co_3(PO_4)_2$@MXene in alkaline seawater.

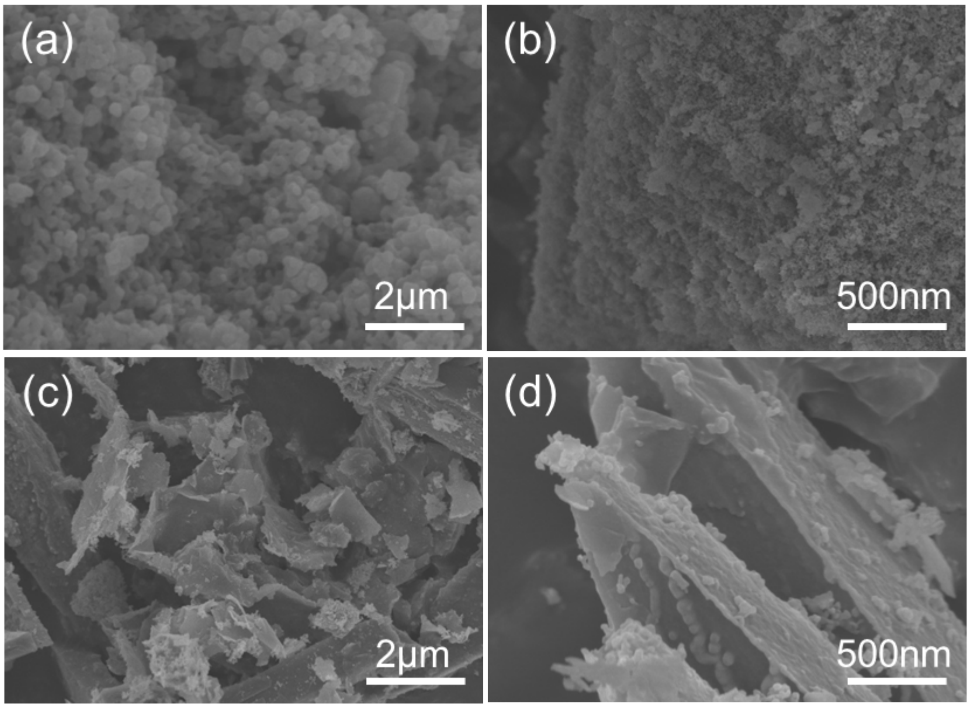

Fig. S8. (a) High-power and (b) low-power SEM images of $Fe_3(PO_4)_2$. (c) High-power and (d) low-power SEM images of $Fe_3(PO_4)_2$@MXene.

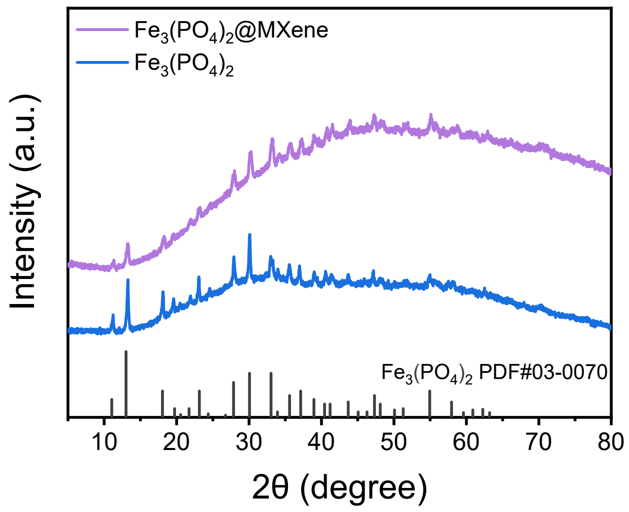

Fig. S9. XRD pattern of $Fe_3(PO_4)_2$ and $Fe_3(PO_4)_2$@MXene.

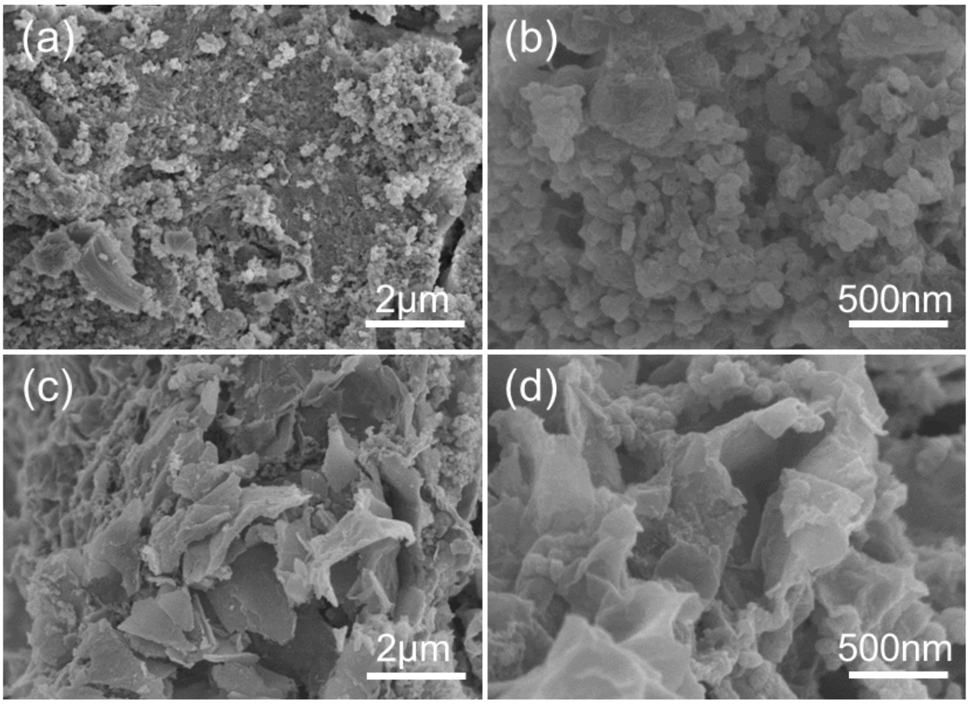

Fig. S10. (a) High-power and (b) low-power SEM images of $Ni_3(PO_4)_2$. (c) High-power and (d) low-power SEM images of $Ni_3(PO_4)_2$@MXene.

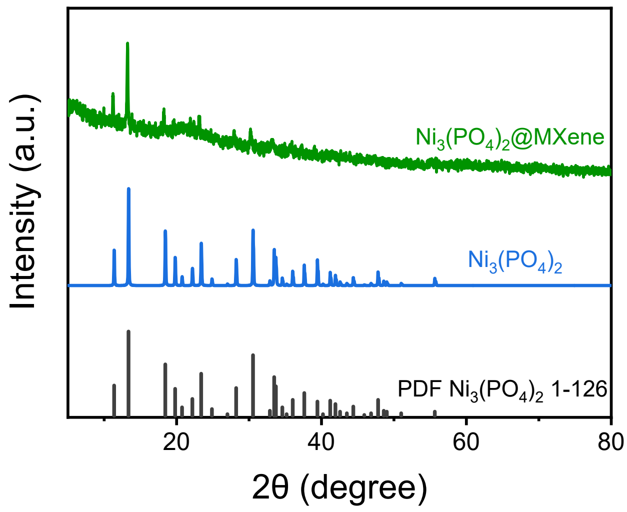

Fig. S11. XRD pattern of $Ni_3(PO_4)_2$ and $Ni_3(PO_4)_2$@MXene.

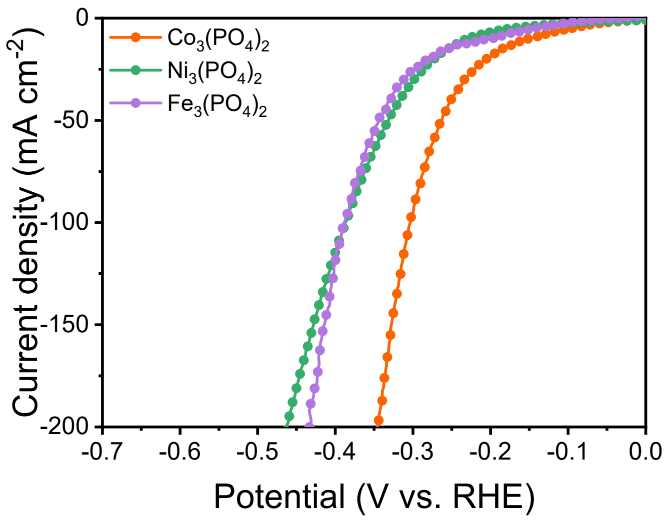

Fig. S12. LSV polarization curve of in of $M_3(PO_4)_2$ (M = Ni, Co, Fe) in 1 M KOH electrolyte.

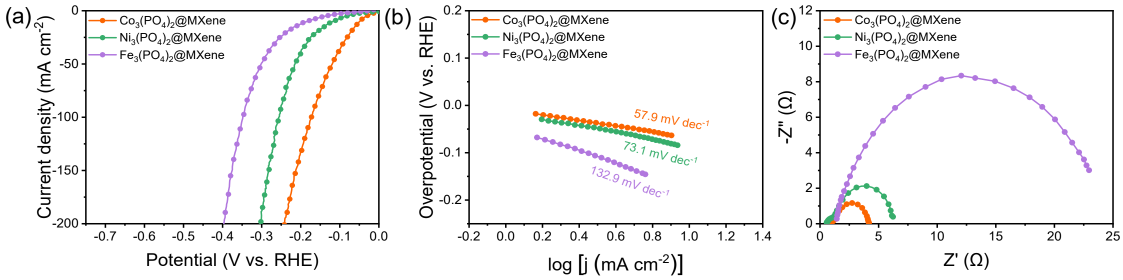

Fig. S13. (a) LSV polarization curve, (b) Tafel slope diagram, and (c) EIS curves of in of $M_3(PO_4)_2$@MXene (M = Ni, Co, Fe) in 1 M KOH electrolyte.

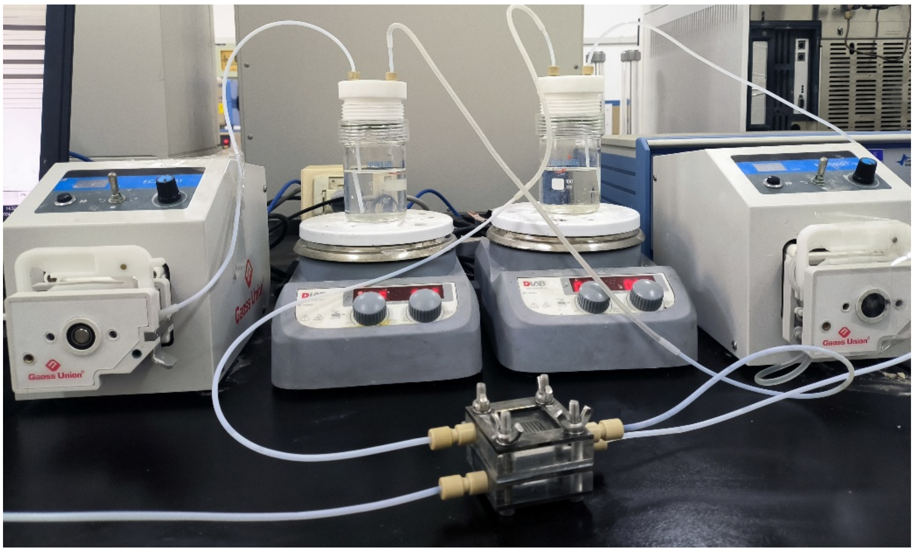

Fig. S14. The two-electrode AEM water electrolyzer.

Table S1. A comparison of HER activity measured for $Co_3(PO_4)_2$@MXene with other representative cobalt-based catalysts reported that HER catalysts used 1 M KOH as an electrolyte.

Catalyst	Overpotential (mV) @10 mA cm^{-2}	Stability (h)	References
$Co_3(PO_4)_2$@MXene	**48**	**100@10 mA cm^{-2} (1 M KOH) 165@500 mA cm^{-2} (1 M KOH seawater)**	**This work**
RuCo-CAT/CC	38	15@10 mA cm^{-2}	Adv. Funct. Mater. 2023, 13, 2204177.
Pt@CoN_4-G	39	12@10 mA cm^{-2}	Adv. Funct. Mater. 2023, 33, 2303189.
NiCoVP	42	30@10 mA cm^{-2}	J. Mater. Chem. A 2021, 9, 12203-12213.
Fe@Co_9S_8-hcp	44.1	20@600 mA cm^{-2}	Adv. Funct. Mater. 2023, 33, 2210298.
NiCoP-WO_x	49	60@10 mA cm^{-2}	J. Mater. Chem. A 2021, 9, 10909-10920.
CuCo-CAT	52	10@10 mA cm^{-2}	Adv. Mater. 2021, 33, 2106781.
CoNiRu-NT_3	52	48@10 mA cm^{-2}	Adv. Mater. 2022, 34, 2107488.
CoF_2	54	110@10 mA cm^{-2}	Adv. Sci. 2022, 9, 2103567.
$CoMo_2S_4$	55	24@100 mA cm^{-2}	Adv. Funct. Mater. 2021, 31, 2103732.

$Co_{3-x}Ni_xO_4$	57	300@20 mA cm^{-2}	ACS Catal. 2021, 11, 8174-8182.
$NiCoRu_{0.2}$/SP	59	100@10 mA cm^{-2}	Appl. Catal. B Environ. 2023, 331, 122710.
10:MoCo-VS_2/CC	63	36@10 mA cm^{-2}	J. Mater. Chem. A 2022, 10, 9067-9079.
V-SRCO	72.3	57@10 mA cm^{-2}	Adv. Energy Mater. 2023, 13, 2301779.
$CoTe_2$/CoP	80	20@100 mA cm^{-2}	Appl. Catal. B Environ. 2023, 329, 122551.
Ce-CoP@CC	81	25@10 mA cm^{-2}	Adv. Energy Mater. 2023, 13, 30.
$NiCo_2S_4/ReS_2$	85	15@10 mA cm^{-2}	Adv. Funct. Mater. 2022, 33, 2210072.
1T Co-$WS_2/NiTe_2$/Ni	88	24@50 mA cm^{-2}	Nano Energy 2022, 102, 107712.
$Co_{0.5}W_{0.5}S_x$	110	10@10 mA cm^{-2}	J. Mater. Chem. A. 2021, 9, 11359-11369.
Fe-Co-Ni MOF	116	48@10 mA cm^{-2}	J. Am. Chem. Soc. 2022, 144, 3411-3428.
Mo-$Co_{0.85}$SeVSe/NC	151	12@100 mA cm^{-2}	Adv. Funct. Mater. 2021, 32, 2109556.
CoP_x/CNS	171	60@16 mA cm^{-2}	Angew. Chem. Int. Ed. 2020, 59, 21360-21366.

Table S2. Comparison of catalytic performance for alkaline seawater electrolysis

Catalyst	Potential (V)	Stability (h)	References
$Co_3(PO_4)_2$@MXene || NiFe LDH	**1.81@100 mA cm^{-2} 2.01@500 mA cm^{-2}**	**165 @500 mA cm^{-2}**	**This work**
CoFe-Ni_2P/Ni-felt || CoFe-Ni_2P/Ni-felt	1.738@100 mA cm^{-2} 1.891@500 mA cm^{-2}	100 @500 mA cm^{-2}	Adv. Energy Mater. 2023, 13, 2301475.
Cr-Co_xP || Cr-Co_xP	1.54@10 mA cm^{-2} 1.85@100 mA cm^{-2} 2.01@200 mA cm^{-2}	16 @100 mA cm^{-2}	Adv. Funct. Mater. 2023, 33, 2214081.
CoP_x || CoP_x@FeOOH	1.71V@100 mA cm^{-2} 1.867@500 mA cm^{-2}	80 @500 mA cm^{-2}	Appl. Catal. B Environ. 2021, 294, 120256.
Ni_2P-Fe_2P/NF || Ni_2P-Fe_2P/NF	1.811@100 mA cm^{-2} 2.004@500 mA cm^{-2}	48 @100 mA cm^{-2} 38 @500 mA cm^{-2}	Adv. Funct. Mater. 2020, 31, 2006484.
BDD|| Cu_2S@NiS@Ni/NiMo	1.68@100 mA cm^{-2} 1.82@500 mA cm^{-2}	2000 @500 mA cm^{-2}	Adv. Energy Mater. 2023, 33, 2302263.
NiMoN || S-(Ni,Fe)OOH	1.661@100 mA cm^{-2} 1.837@500 mA cm^{-2}	100 @100 mA cm^{-2} 100 @500 mA cm^{-2}	Energy Environ. Sci. 2020, 13, 3439-3446.
N-CDs/NiFe || LDH/NF	1.56@100 mA cm^{-2}	20 @10 mA cm^{-2}	Nano Res. 2022, 15, 7063-7070.

Table S3. Comparison of catalytic performance for alkaline water/seawater electrolysis in $Co_3(PO_4)_2$@MXene || NiFe LDH electrolyzer.

Catalyst	Potential (V)	Stability (h)	References
$Co_3(PO_4)_2$@MXene || NiFe LDH	**1.71@500 mA cm^{-2} 2.0@1000 mA cm^{-2}**	**50 @500 mA cm^{-2}**	**This work**
CoFe-Ni_2P/Ni-felt || CoFe-Ni_2P/Ni-felt	2.25@1 A cm^{-2} 2.79@3 A cm^{-2} (6 M KOH seawater)	350 @1 A cm^{-2}	Adv. Energy Mater. 2023, 13, 2301475.
NiFe@DG || Pt/C	1.496@10 mA cm^{-2} 1.602@100 mA cm^{-2} (1 M KOH seawater)	1000 @10 mA cm^{-2}	ACS Nano 2023, 17, 18372-18381.
Ni-MoN || SSM	1.635@100 mA cm^{-2} 1.783@500 mA cm^{-2} (1 M KOH seawater)	100 @100 mA cm^{-2} 100 @500 mA cm^{-2}	Adv. Mater 2022, 34, 2201774.
	1.613@100mA cm^{-2} 1.7@500 mA cm^{-2} (1 M KOH)	/	
NiMoN || NiMoN@NiFeN	1.581@100 mA cm^{-2} 1.77@500 mA cm^{-2} (1 M KOH seawater)	100 @100 mA cm^{-2} 100 @500 mA cm^{-2}	Nat. Commun. 2019, 10, 5106.
NiP_2-FeP_2/Cu_{NW}/CF || NiFe-LDH/NF	1.76@100 mA cm^{-2} (1 M KOH) 1.93@100 mA cm^{-2} (1 M KOH + 0.6 M NaCl)	/	ACS Energy Lett. 2021, 6, 354.